Multifractal behavior of nuclear fragments in high-energy leptonic interactions

Dipak Ghosh, Argha Deb, Madhumita Banerjee Lahiri, Parthasarathi Ghosh, Syed Imtiaz Ahmed, and Prabir Kumar Halder
Nuclear and Particle Physics Research Centre, Department of Physics, Jadavpur University, Kolkata 700032, India
(Received 29 December 2003; published 5 November 2004)

The multifractal analysis of nuclear fragmentation data obtained from muon-nucleus interactions at 420 ± 45 GeV is performed using G-moment and Takagi-moment methods. The generalized fractal dimensions D_q are determined from these methods and also are compared with those obtained from intermittency exponents. The analysis reveals the multifractal behavior of target fragments in lepton-nucleus interactions.

DOI: 10.1103/PhysRevC.70.054903 PACS number(s): 24.60.Ky, 25.30.−c, 25.70.Pq, 25.75.−q

I. INTRODUCTION

To search for the dynamical origin of large local fluctuations in a single event of very high multiplicity recorded by the JACEE Collaboration [1], the anomalous scaling of factorial moments with phase space bin size called intermittency has been proposed by Bialas and Peschanski [2]. Such a kind of anomalous scaling has recently been observed in various experiments [3–7]. The concept of intermittency is in turn intimately connected to the fractal geometry of the underlying physical process [8]. Mandelbrot [9], the pioneer, showed a new way of looking into the world of apparent irregularities or fractals. Fractal geometry allows us to mathematically describe systems that are intrinsically irregular at all scales. A fractal structure has the property that if one magnifies a small portion of it, this shows the same complexity as the entire system. The idea is therefore to construct a formalism that is able to describe systems with local properties of the self-similarity. Different methods have been proposed for studying the fractal structures in multiparticle data [10–14].

The most notable property of fractals is their dimensions [15]. We have used two different methods for extracting the fractal dimensions: the G-moment method [12–14,16] and Takagi-moment method [17].

The G moments are constructed to reveal the fractal properties of the multiplicity distribution by Hwa and others [12,16]. These G moments are, however, dominated by statistical fluctuations when the event multiplicity is very low. Hwa and Pan modified the old form of the G moments by introducing a step function, which can act as a filter for the low-multiplicity events.[10,11,16,18]

Recently Takagi[17] proposed a novel method for studying the fractal structure where the difficulties faced in the conventional methods have been overcome. Takagi has pointed out that in the common methods the experimental data do not show the expected linear behavior in a log-log plot, and this is partially due to the fact that most of the methods are unable to satisfy the required mathematical limit, the number of points tends to infinity.

These two methods have their own merits and demerits, yet these are the most widely accepted methodologies for extracting the fractal dimensions in studies of multiparticle production.

Multifractality has become the focal point of a number of theoretical and experimental investigations in high-energy nuclear collisions [12,13,16,18,19] in order to discern the proper dynamics of multiparticle production. Most of the investigations on multifractality have been carried out on the produced pions with the common belief that they are the most informative about the collisional dynamics. Analysis of target-associated particles that manifest themselves as gray and black tracks in emulsion experiments in high-energy interactions is scanty. In fact, whatever knowledge we have about these particles is based on hadron-emulsion and heavy-ion–emulsion interactions and suggests that the gray and black tracks are of the same origin in the emulsion. The black tracks, of interest to us in the present analysis, are identified as target evaporation particles in a model referred to as the "evaporation model" [20].

In the evaporation model, the shower and gray tracks are emitted from the nucleus very soon after the instant of impact, leaving the hot residual nucleus in an excited state. Emission of black particles from this state takes place relatively slowly [21]. In order to escape from this residual nucleus, a particle must await a favorable situation. Random collisions between the nucleons within the nucleus sometimes take the particle close to the nuclear boundary, traveling in an outward direction and with a kinetic energy greater than the binding energy of the nucleus. After the evaporation of this particle, a second particle is brought to the favorable condition for evaporation and so on, until the excitation energy of the residual nucleus becomes very small. After that, transition to the ground state is likely to be affected by the emission of the γ rays only. In the rest system of the nucleus in this model, the directions of the emission of the evaporation particles are distributed isotropically. In different experiments, however, the isotropicity has been found to be disturbed, which may be due to the loss of kinetic energy of the residual nucleus through ionization, following the impulse of collision, before the evaporation process is completed. The evaporation model is based on the assumption that statistical equilibrium has been established in the decaying system and that the lifetime of the system is much longer than the time taken to distribute the energy among the nucleons in the nucleus.

This model is not free of irregularities. Takibaev *et al.* and Adamovich *et al.*, analyzing the experimental data of proton emulsion experiments at the incident energies 67–400 GeV [22], observed the dominance of nonstatistical fluctuation over the statistical part in angular distribution of "black" particles. In this recent study also, the angular distribution of black particles from muon-nucleus interactions could not be explained very satisfactorily by the evaporation model. Results from our analyses of fragmentation data of muon-nucleus interactions at 420±45 GeV in terms of scale factorial moments [23] and also the possibility of the existence of nonequilibrium processes of emission of slow, target-associated particles motivate us to use the *G* moments and Takagi (*T*) moments as a diagnostic tool of the dynamical phenomenon, in analyzing the angular distribution of these so-called "target-evaporation particles."

The present paper reports the results of analysis of the angular distribution of the target fragments emitted from muon-nucleus interactions in terms of the *T* and *G* moments. No doubt it would be interesting to explore for the first time if the emission process of the target-evaporated slow particles in the case of lepton-nucleus interactions also exhibits a multifractal structure. This investigation has been done in emission angle space as well as in azimuthal angle space.

II. EXPERIMENTAL DETAILS

The fractal study is performed with the help of the emulsion technique because of the high spatial resolution with 4∂ geometry.

A. Exposure

In this emulsion experiment we have exposed stacks of G5 nuclear emulsion plates to the main muon beam at 420±45 GeV at the Fermi Laboratory (USA) [24]. The emulsions were allowed to warm to room temperature for 4 h before the exposure. The two boxes were leveled to about ±2 mrad. The beam intensity on the emulsion was monitored with a scintillator telescope with a circular aperture of 1.25 cm (in more detail, a counter with a 1.25-cm-diam hole in anticoincidence with two counters $2.5 \times 2.5\ \mathrm{cm}^2$). The density of the integrated exposure is $0.98 \times 10^6\ \mathrm{muons/cm}^2$ at the center, tapering off quadratically to 0.60 at 5 cm from the center (the edge of the emulsion sheets). The beam was deliberately defocused with quadrupoles to get a fairly even density on all parts of the emulsion.

B. Scanning and measurement

The scanning of the events was done with the help of a high-resolution Leitz metalloplan microscope provided with an on-line computer system using objectives 10× in conjunction with a 10× ocular lens. The scanning is done by independent observers to increase the scanning efficiency, which turns out to be 98%.

Criteria for selecting the events were

(i) The events within 20 μm thickness from the top or bottom surface of the plates were not analyzed.

(ii) The beam track did not exceed 3° from the mean beam direction in the pellicle.

(iii) Following the above selection procedure, we have chosen 353 events from our sample plates of muon-nucleus interactions.

All the tracks of each event are classified as usual:

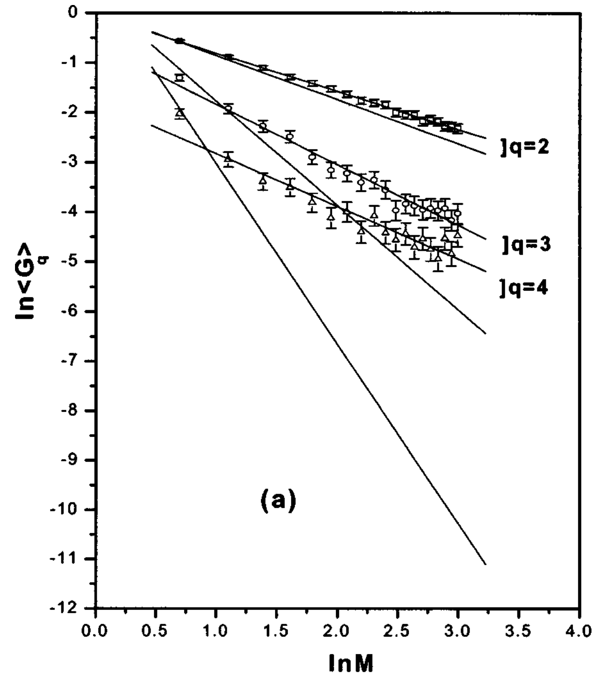

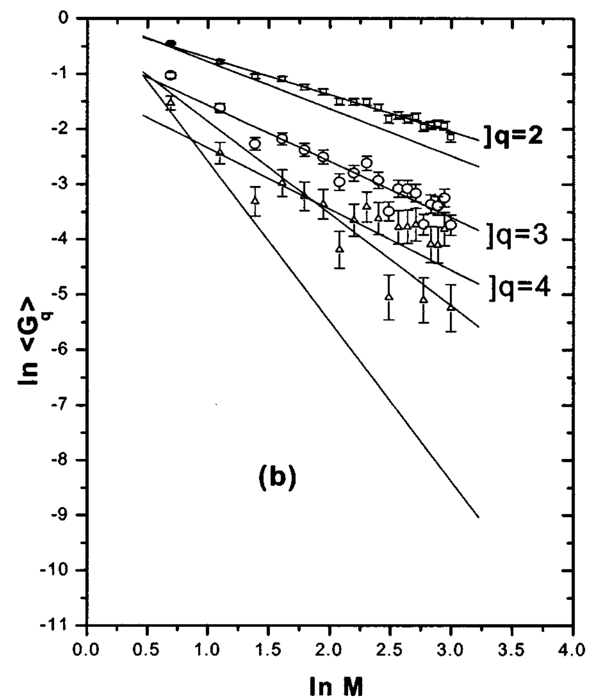

FIG. 1. The dependence of $\ln\langle G_q\rangle$ on $\ln M$ for order $q=2,3,4$ in (a) $\cos\theta$ space and (b) ϕ space for muon-nucleus interactions at 420±45 GeV.

(a) The target fragments with ionization $>1.4I_0$ (I_0 is the plateau ionization) produced either black or gray tracks. The black tracks with range <3 mm represent target evaporation (the light nuclei evaporated from the target) of $\beta<0.3$, singly or multiply charged particles.

(b) The gray tracks with a range $\geqslant 3$ mm and having velocity $0.7\geqslant\beta\geqslant 0.3$ are mainly images of target recoil protons of the energy range up to 400 MeV.

TABLE I. Parameters of the G-moment analysis for $q=2,3,4$ in $\cos\theta$ space.

q	τ_q	τ_q^{stat}	τ_q^{dyn}	D_q^{dyn}
2	0.77 ± 0.009	0.89 ± 0.019	0.88 ± 0.021	0.88 ± 0.021
3	1.21 ± 0.049	2.10 ± 0.082	1.11 ± 0.095	0.56 ± 0.047
4	1.06 ± 0.081	3.62 ± 0.174	0.44 ± 0.191	0.15 ± 0.063

(c) The relativistic shower tracks with ionization $<1.4I_0$ are mainly produced by pions and are not generally confined within the emulsion pellicle. They are believed to carry important information about the nuclear reaction dynamics.

The azimuthal angle (ϕ) and the emission angle (θ) in the laboratory frame of all the black tracks are calculated by taking the readings of the space coordinates (x,y,z) of a point on the track, another point on the incident beam, and the production point by using oil immersion objectives ($100\times$ in conjunction with a $10\times$ ocular lens). The detailed characteristics for each event were obtained. The emulsion technique possesses the highest spatial resolution and thus is the most effective for this type of analysis.

III. THE *G*-MOMENT ANALYSIS

The selected phase-space interval of length x has been divided in to M bins of equal size, the width of each bin being $\delta x = x/M$, n being the total multiplicity of target-associated slow particles in the x interval. Let n_m be the multiplicity of the particles distributed in the mth bin. When M is large, some bins may have no particles (i.e., "empty bins"). Let M' be the number of nonempty bins, which constitute a set of bins that have fractal properties. Hwa proposed a set of fractal moments, G_q, defined as [13]

$$G_q = \sum_{m=1}^{M'} P_m^q, \tag{1}$$

where $P_m = n_m/n$ with $n=\Sigma_{m=1}^{M'} n_m$ and q is the order number. The summation is carried over the nonempty bins only, so that q can cover the whole spectrum of real numbers.

In an attempt to circumvent the problem of statistical noise, Hwa and Pan [16] proposed a modified definition of the G moment as

TABLE II. Parameter of the G-moment analysis for $q=2,3,4$ in ϕ space.

q	τ_q	τ_q^{stat}	τ_q^{dyn}	D_q^{dyn}
2	0.67 ± 0.022	0.86 ± 0.019	0.81 ± 0.029	0.81 ± 0.029
3	1.02 ± 0.077	1.67 ± 0.036	1.35 ± 0.085	0.67 ± 0.042
4	1.11 ± 0.185	2.90 ± 0.243	1.21 ± 0.305	0.40 ± 0.102

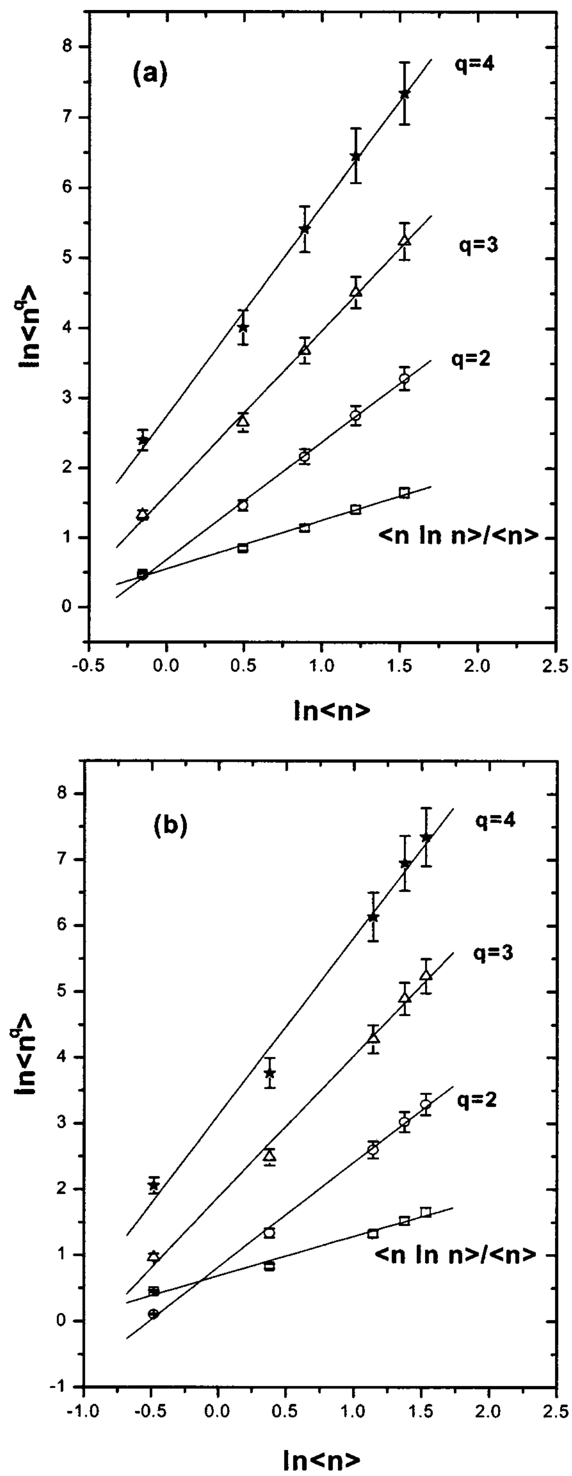

FIG. 2. The dependence of $\ln\langle n^q\rangle$ and $\langle n\ln n\rangle/\langle n\rangle$ on $\ln\langle n\rangle$ for order $q=2,3,4$ in (a) $\cos\theta$ space and (b) ϕ space for muon-nucleus interactions at 420 ± 45 GeV.

$$G_q = \sum_{m=1}^{M'} P_m^q \Theta(n_m - q), \tag{2}$$

where $\Theta(n_m - q)$ is the usual step function that has been added to the old definition in order to filter statistical noise:

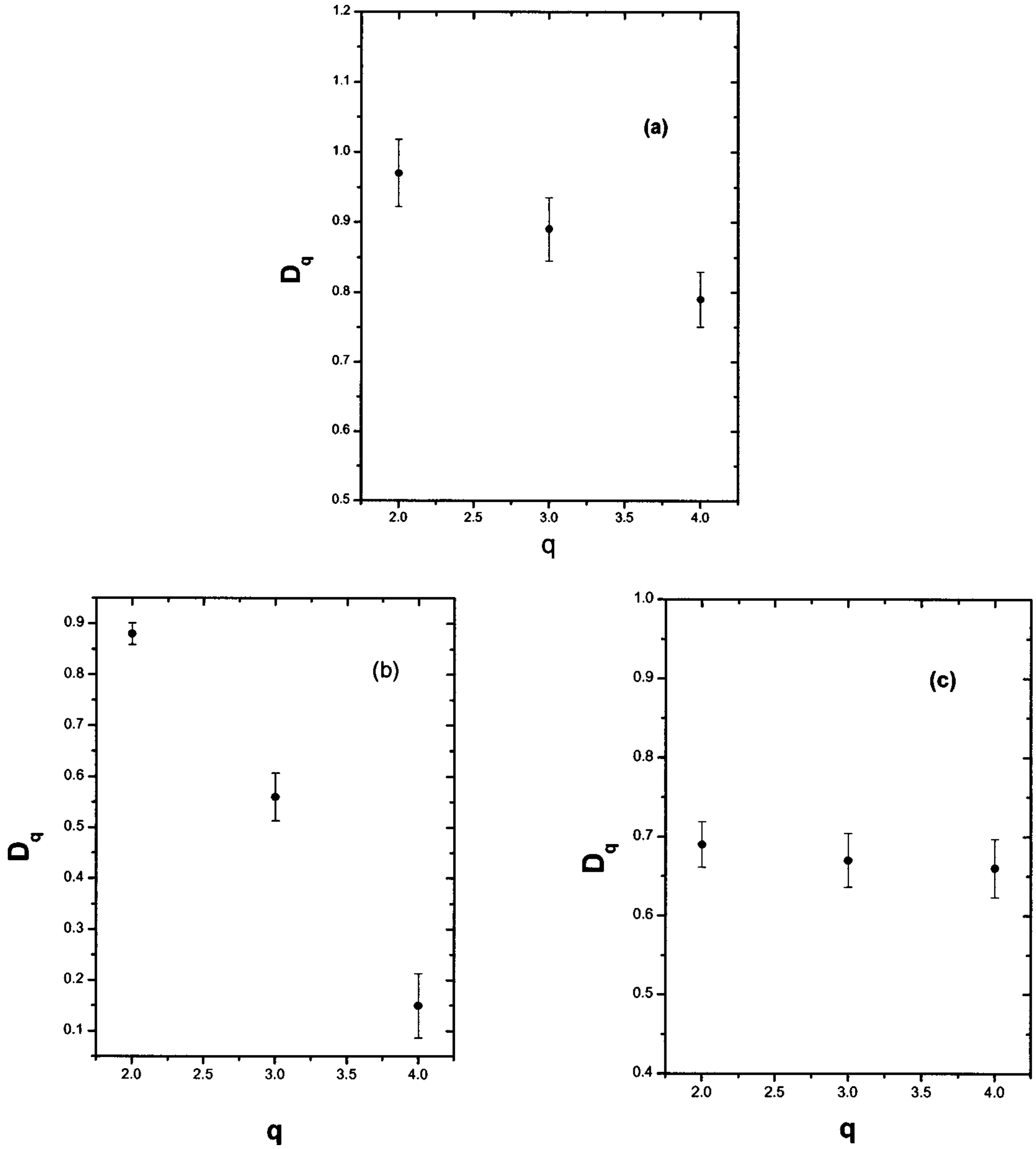

FIG. 3. The q dependence of generalized dimension D_q in $\cos\theta$ space obtained from (a) factorial-moment analysis, (b) G-moment analysis, (c) Takagi-moment analysis.

$$\Theta(n_m - q) = \begin{cases} 1 & \text{if } n_m \geqslant q \\ 0 & \text{if } n_m < q \end{cases} .$$

For very large multiplicity $n/M \gg q$, the step function is essentially unity and so the two definitions coincide. But in the case of target fragmentation, n is a relatively small number and the E function exerts a crucial influence on the G moments. It imposes a nonanalytical cutoff at positive integer values of q. Thus is the real environment of high-energy collisions, where the multiplicity is rather low and the G moments are dominated by statistical fluctuactions.

For an ensemble of events, the averaging is done as

$$\langle G_q \rangle = \frac{1}{\Omega} \sum G_q, \tag{3}$$

where Ω is the total number of events in the ensemble. According to the theory of multifractals, a self-similar particle emission process is characterized by a power law behavior [13,14],

$$\langle G_q \rangle \propto M^{-\tau_q}, \tag{4}$$

where τ_q is the fractal index and can be obtained from the slope of the $\ln\langle G_q(M)\rangle$ versus $\ln M$ plot:

$$\tau_q = \delta \ln \langle G_q(M)\rangle / \delta \ln (M). \tag{5}$$

We have divided the $\cos\theta$ space and ϕ space into $M = 2,3,4,\ldots,20$ bins. For each event we have calculated the G moments of order $q=2,3,4$ using Eq. (2). The logarithm of event-averaged G moments of the order $q=2,3,4$ have been plotted against $\ln M$ in Figs. 1(a) and 1(b) in emission angle space ($\cos\theta$ as the phase-space variable) and azimuthal angle space (ϕ as the phase-space variable), respectively. A linear dependence of $\ln\langle G_q\rangle$ on $\ln M$ is observed, indicating self-similarity in the particle emission process.

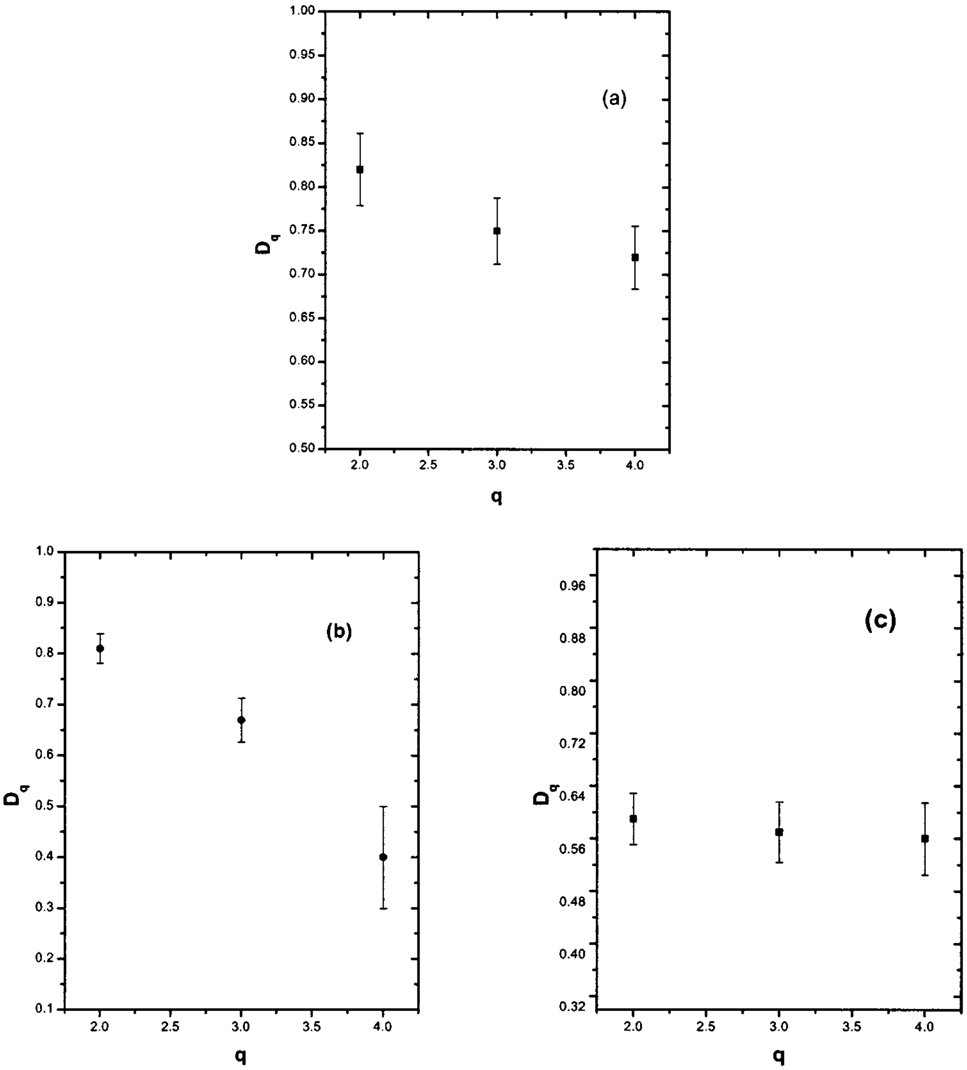

FIG. 4. The q dependence of generalized dimension D_q in ϕ space obtained from (a) factorial-moment analysis, (b) G-moment analysis, (c) Takagi-moment analysis.

The exponent τ_q of the power-law behavior is obtained by a linear least-square fitting of the data points. The values are listed in Tables I and II for the cos θ and ϕ space, respectively.

For the estimation of statistical contribution to $\langle G_q \rangle$, we distribute n particles randomly in the considered interval, and using the same procedure we calculate $\langle G_q^{\rm st} \rangle$ as in Eq. (3) and $\tau_q^{\rm st}$ as in Eq. (5). The best-fitted lines for $\ln\langle G_q^{\rm st} \rangle$ versus $\ln M$ plots are shown by the solid lines in Figs. 1(a) and 1(b). The slopes $\tau_q^{\rm st}$ are listed in Tables I and II correspondingly. The dynamical component of $\langle G_q \rangle$ can be estimated from the formula given by Chiu, Fialkowaski, and Hwa [25],

$$\langle G_q \rangle^{\rm dyn} = [\langle G_q \rangle / \langle G_q^{\rm st} \rangle] M^{1-q},$$

which gives

$$\tau_q^{\rm dyn} = \tau_q - \tau_q^{\rm st} + q - 1. \tag{6}$$

If $\langle G_q \rangle$ is purely statistical, then $\langle G_q \rangle^{\rm dyn}$ is M^{1-q}, which is the result for trivial dynamics. Under such a condition $\tau_q^{\rm dyn} = q - 1$. Any deviation of $\tau_q^{\rm dyn}$ from $q-1$ indicates the presence of dynamical information.

A relation between the G_q moment and the F_q moment has been developed [16], thus providing a fractal interpretation for intermittency. The fractal index τ_q measures the strength of multifractality, while the intermittency index α_q is a measure of the strength of the intermittency. Thus, a correspondence between intermittency and multifractality can be obtained by relating the indices α_q and τ_q. The two indices have been shown to be approximately related as [16]

$$\alpha_q \approx q - 1 - \tau_q^{\rm dyn}. \tag{7}$$

The relationship is not exact because F_q and G_q are different moments and approach each other only in the limiting case of infinite multiplicity. It is clear from Eq. (7) that the deviation of α_q from zero is equivalent to the deviation of $\tau_q^{\rm dyn}$ from $q-1$. Thus to compare the fractal behavior of $\langle F_q \rangle$ and $\langle G_q \rangle$, we should compare α_q and $q-1-\tau_q^{\rm dyn}$.

We have plotted the value for α_q (solid circles) and the value for $q-1-\tau_q^{\rm dyn}$ (open circles) with the order q in Figs. 2(a) and 2(b) for the cos θ and ϕ space, respectively. It is observed from these figures that in each case the two values α_q and $q-1-\tau_q^{\rm dyn}$ are not equal, but both of them increase with the order q.

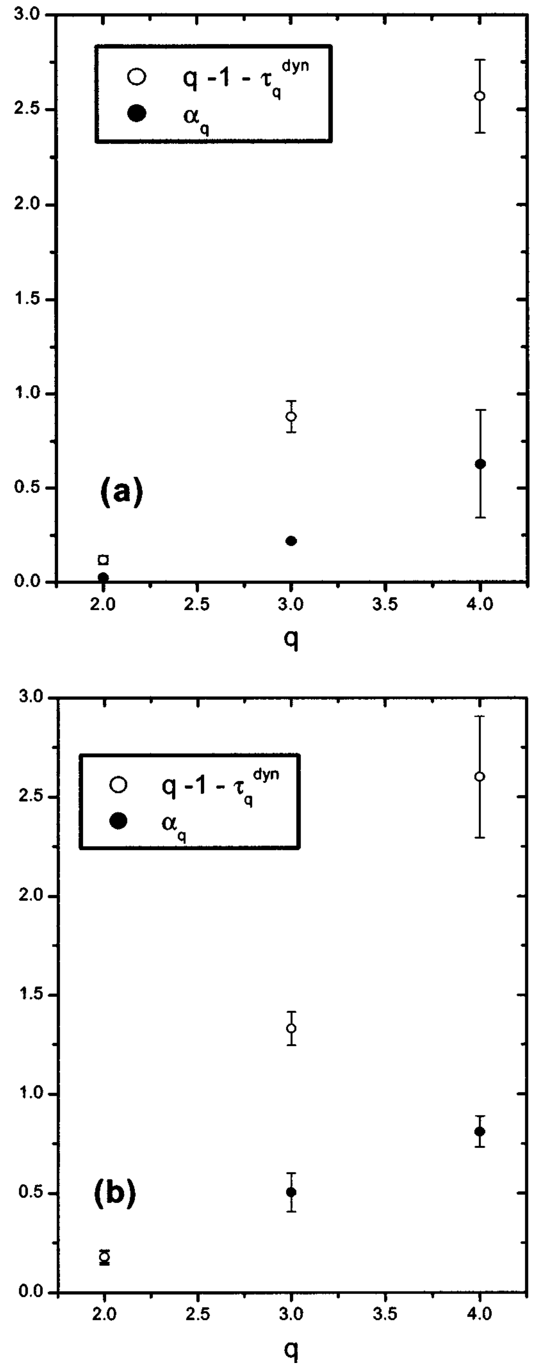

FIG. 5. Comparison of F and G moments in (a) cos θ and (b) ϕ space.

The generalized fractal (Renyi) dimensions are obtained from the relation

$$D_q^{\mathrm{dyn}} = \tau_q^{\mathrm{dyn}}/(q-1). \tag{8}$$

For muon-nucleus interactions at 420 ± 45 GeV, the values of D_q^{dyn} have been calculated using Eqs. (6) and (8) and are listed in Tables I and II for the cos θ and ϕ space, respectively. The corresponding values of τ_q, τ_q^{st}, and D_q^{dyn} are also included in Tables I and II.

TABLE III. Comparative study of generalized fractal dimensions in the cos θ space obtained from different methods.

Order of moment q	D_q		
	F_q moment	G_q moment	T_q moment
2	0.97 ± 0.048	0.88 ± 0.021	0.69 ± 0.029
3	0.89 ± 0.045	0.56 ± 0.047	0.67 ± 0.034
4	0.79 ± 0.039	0.15 ± 0.063	0.66 ± 0.037

IV. THE TAKAGI-MOMENT ANALYSIS

Consider a single event that contains n particles. The multiplicity n changes from event to event according to the distribution $P_n(x)$. The selected phase-space interval of length Δx has been divided to M bins of equal size, the width of each bin being $\delta x = \Delta x / M$. Then the multiplicity distribution for a single bin is denoted as $P_n(\delta x)$ for $n = 0, 1, 2, 3 \ldots$, where we assume that the inclusive particle distribution dn/dx is constant and $P_n(\delta x)$ is independent of the location of the bin. n particles contained in a single event is distributed in the interval $x_{\min} < x < x_{\max}$. The multiplicity n changes from event to event according to the distribution $P_n(\Delta x)$, where $\Delta x = x_{\max} - x_{\min}$. If the number of independent events is Ω, then the particles emitted from those events are distributed in ΩM bins of size δx. Let N be the total number of target-associated slow particles produced in these Ω events and n_{aj} the multiplicity of black particles in the jth bin of the ath event.

The theory of multifractals [26,27] motivates one to consider the normalized density P_{aj} defined by $P_{aj} = n_{aj}/N$. This is of course also true when $N \to \infty$. Then one has to consider the quantity

$$T_q(\delta x) = \ln \sum_{a=1}^{\Omega} \sum_{j=1}^{M} P_{aj}^q \quad \text{for } q > 0,$$

which behaves like a linear function of the logarithm of the "resolution" $R(\delta x)$, and q is the order number.

$$T_q(\delta x) = A_q + B_q \ln R(\delta x),$$

where A_q and B_q are constants independent of δx. If such a behavior is observed for a considerable range of $R(\delta x)$, a generalized dimension may be determined as

$$D_q = B_q/(q-1). \tag{9}$$

Now evaluating the double sum of P_{ij}^q for sufficiently large Ω, Takagi [17] expects a linear relation

$$\ln\langle n^q \rangle = A_q + (B_q + 1)\ln R(\delta x).$$

While analyzing real data [28] it was observed [29] that plot of $\ln\langle n^q \rangle$ against δx saturates for the large-x region. This deviation may be due to the nonflat behavior of dn/dx in the large-x region. Bailas and Gazdzicki and also Takagi suggested that $\langle n \rangle$ would be a better choice of the "resolution" $R(\delta x)$ because $dn/d\langle n \rangle$ is flat by definition [26,29]. Choosing $R(\delta x) = \langle n \rangle$ one has

TABLE IV. Comparative study of generalized fractal dimensions in the ϕ space obtained from different methods.

	D_q		
Values of q's	F_q moment	G_q moment	T_q moment
2	0.82 ± 0.041	0.81 ± 0.029	0.59 ± 0.039
3	0.75 ± 0.038	0.67 ± 0.043	0.57 ± 0.046
4	0.72 ± 0.036	0.40 ± 0.102	0.56 ± 0.055

$$\ln\langle n^q \rangle = A_q + (B_q + 1)\ln\langle n \rangle, \tag{10}$$

a simple linear relation between $\ln\langle n^q \rangle$ and $\ln\langle n \rangle$. The generalized dimension D_q can be obtained from the slope values using Eq. (9).

The case with $q=1$ can be obtained by taking an appropriate limit [27]. The value of information dimension D_1 can also be determined from a new and simple relation suggested by Takagi [17],

$$\langle n \ln n \rangle / \langle n \rangle = C_1 + D_1 \ln\langle n \rangle, \tag{11}$$

where C_1 is a constant.

In the present case the cosine of emission angle of black-track interval ($\Delta \cos \theta = 1$) is divided into overlapping bins, whose size is increased symmetrically in steps of 0.2 around the central value 0 (zero) and the azimuthal angle interval ($\boldsymbol{\Delta\Phi} = 360°$) is divided into overlapping bins, whose size is increased symmetrically in steps of 20° around the central value 180°. For each bin we have calculated $\langle n^q \rangle$ and $\langle n \ln n \rangle / n$ for both spaces. Figures 3(a) and 3(b) represent the nature of the variation of $\ln\langle n^q \rangle$ (for $q=2,3,4$) and $\langle n \ln n \rangle / \langle n \rangle$ with $\ln\langle n \rangle$ for $\cos \theta$ as the phase-space variable and ϕ as the phase-space variable, respectively. All the plots show excellent linear behavior. We have performed best linear fits to the experimental data points and have calculated the values of generalized dimensions D_q ($q=2,3,4$) using Eqs. (9) and the value of information dimension D_1 using Eq. (11) (Figs. 4 and 5).

Table III presents the values of generalized dimensions D_q obtained from the G-moment, T-moment, and also from F-moment methods (from our earlier work [23]) for the $\cos \theta$ space. Table IV presents the corresponding values of generalized dimensions D_q for ϕ space.

V. CONCLUSIONS

In this paper we have made an attempt to study the fractality and to extract the fractal dimension of target fragmentation processes in muon-nucleus interactions at 420 ± 45 GeV. One should appreciate the fact that it is very difficult to extract the exact fractal dimension in an unambiguous way. However, there exist three different approaches (F moment, G moment, and T moment) for extracting the fractal dimension. We have already pointed out earlier that each method has its own merits and demerits. It has been observed in the works of different groups [30–32] that different methods give different values of fractal dimension. The present analysis also does not show any exception in this regard. Nevertheless, it is interesting to note that each method shows a decrease of fractal dimension with the order of moment indicating multifractal nature of the fragmentation process in both $\cos \theta$ space and ϕ space. One should note the rationale behind the analysis in two phase spaces. Since the analysis in one phase space ($\cos \theta$) can give restricted information of the fluctuation pattern of the emission process, it is essential to study in other phase spaces, i.e., in the azimuthal angle space (ϕ) also, to have a clear idea of multifractal nature of the slow target-evaporated particles.

[1] T. H. Burnet *et al.*, Phys. Rev. Lett. **50**, 2062 (1983).
[2] A. Bialas and R. Peschanski, Nucl. Phys. **273**, 703 (1986); **308**, 857 (1988).
[3] E. A. De Wolf, I. M. Demin, and W. Kittel, Phys. Rep. **270**, 1 (1996).
[4] NA22 Collaboration, N. M. Agababyan *et al.*, Phys. Lett. B **382**, 305 (1996); **431**, 451 (1998).
[5] S. Wang, Z. Wang, and C. Wu, Phys. Lett. B **410**, 323 (1997).
[6] D. Ghosh, A. Deb, and M. Lahiri, Phys. Rev. D **51**, 3298 (1995).
[7] D. Ghosh *et al.*, Z. Phys. C **71**, 243 (1996).
[8] C. B. Chiu and R. C. Hwa, Phys. Rev. D **45**, 2276 (1992).
[9] B. B. Mandelbrot, *The Fractal Geometry of Nature* (Freeman, New York, 1982).
[10] I. M. Dremin, Mod. Phys. Lett. A **3**, 1333 (1988).
[11] P. Carruthers, Int. J. Mod. Phys. A **4**, 5587 (1989).
[12] Ph. Brax and R. Peschanski, Nucl. Phys. **B346**, 65 (1990); N. G. Antoniou *et al.*, Phys. Rev. D **45**, 4034 (1992).
[13] R. C. Hwa, Phys. Rev. D **41**, 1456 (1990).
[14] C. B. Chiu and R. C. Hwa, Phys. Rev. D **43**, 100 (1991); W. Florkowski and R. C. Hwa, *ibid.* **43**, 1548 (1991).
[15] G. Paladin and A. Vulpiani, Phys. Rep. **156**, 147 (1987).
[16] R. C. Hwa and J. C. Pan, Phys. Rev. D **45**, 1476 (1992).
[17] F. Takagi, Phys. Rev. Lett. **72**, 32 (1994).
[18] L. P. Jain, K. Sengupta, and G. Sing, Phys. Lett. B **241**, 273 (1990); EMC Collaboration, T. Derado *et al.*, Phys. Lett. B **283**, 151 (1992); UA1 Collaboration, C. Albajar *et al.*, Z. Phys. C **56**, 37 (1992); UA1 Collaboration, H. Dibon *et al.*, paper submitted to the XXVI Int. Conf. on High Energy Physics, Dallas, USA, 1992.
[19] D. Ghosh *et al.*, Phys. Lett. B **272**, 5 (1991).
[20] C. F. Powell, P. H. Fowler, and D. H. Perkins, *The Study of Elementary Particles by the Photographic Method* (Oxford, Pergamon, 1959), pp. 450–464 and references therein.
[21] E. Sterlund and I. Otterlund, Nucl. Phys. **B198**, 407 (1982).
[22] S. Zh. Takibaev *et al.*, Sov. J. Nucl. Phys. **47**, 282 (1988); KMU-01 Collaboration, I. M. Adamovich *et al.*, Phys. Lett. B **262**, 369 (1991).

[23] D. Ghosh *et al.*, Fiz. B **11**, 3 (2002); D. Ghosh *et al.*, Indian J. Phys., A **78**, 363 (2004).

[24] L. Chatterjee, D. Ghosh, and T. Murphy, *Hyperfine Interaction* (J. C. Balzer AG, Science Publishers, 1993), p. 1034.

[25] C. B. Chiu, K. Fialkowaski, and R. C. Hwa, Mod. Phys. Lett. A **5**, 2651 (1990).

[26] A. Bailas and M. Gazdzicki, Phys. Lett. B **252**, 483 (1990).

[27] H. G. E. Hentschel and I. Procaccia, Physica D **8**, 435 (1983).

[28] Tasso Collaboration, W. Braunschweig *et al.*, Z. Phys. C **45**, 159 (1989); DELPHI Collaboration, P. Abreu *et al.*, *ibid.* **52**, 271 (1991); UA5 Collaboration, R. E. Ansorge *et al.*, *ibid.* **43**, 357 (1989).

[29] F. Takagi, Phys. Rev. Lett. **53**, 427 (1984); Phys. Rev. C **32**, 1799 (1985).

[30] R. Hasan, M. Mohib-ul Haq, and Saiful Islam, Int. J. Mod. Phys. E **9**, 417 (2000), and references therein.

[31] D. Ghosh *et al.*, Fractals **11**, 331 (2003).

[32] P. L. Jain and G. Singh, Phys. Rev. C **44**, 854 (1991).